

Fig. 1 Equivalent circuit of a solar panel connecting to a converter.

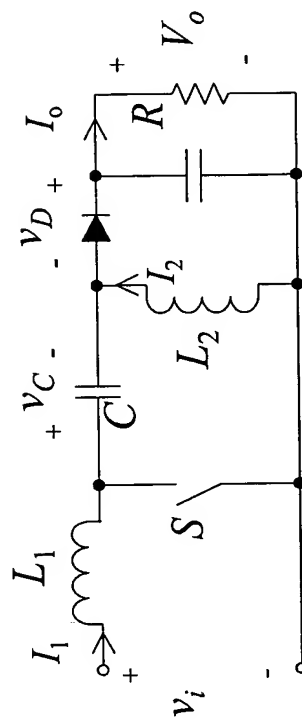


Fig. 2 SEPIC converter circuit.

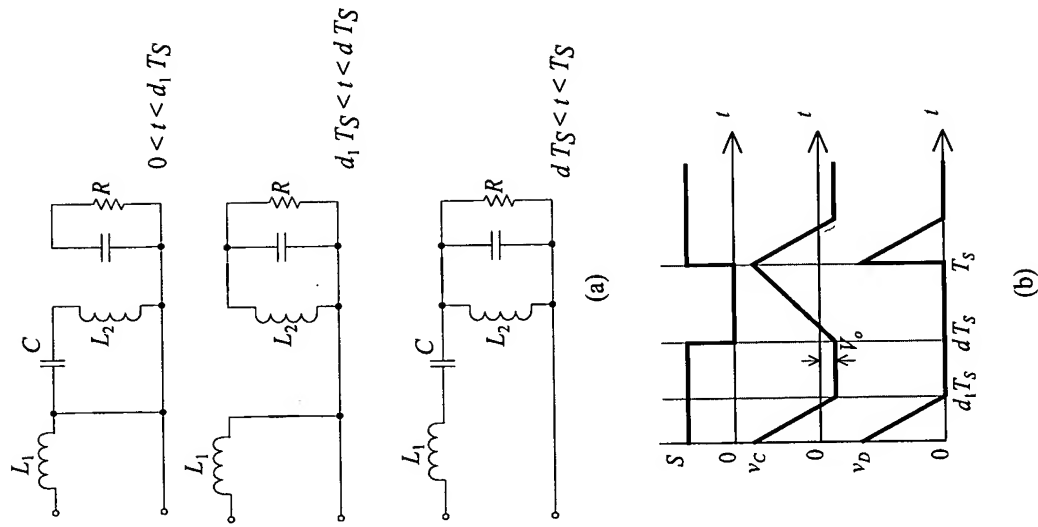


Fig. 3 Operating principle. (a) Topology sequence. (b) Theoretical waveforms of  $v_C$  and  $v_D$ .

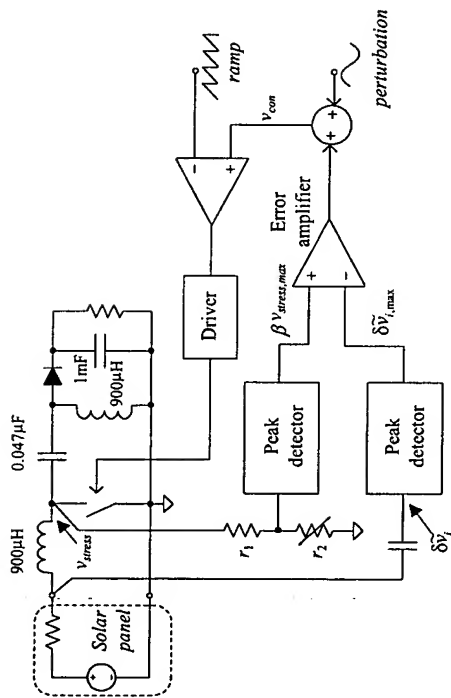


Fig. 4 Block diagram of proposed MPP tracking method.

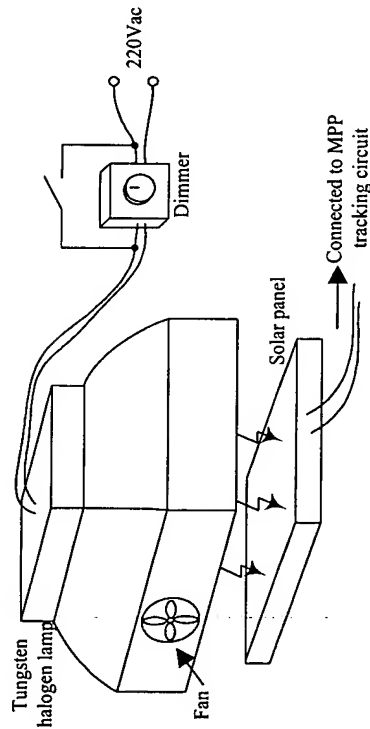
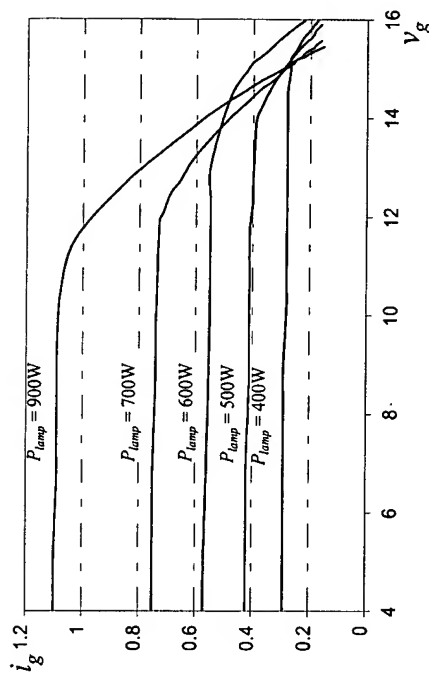
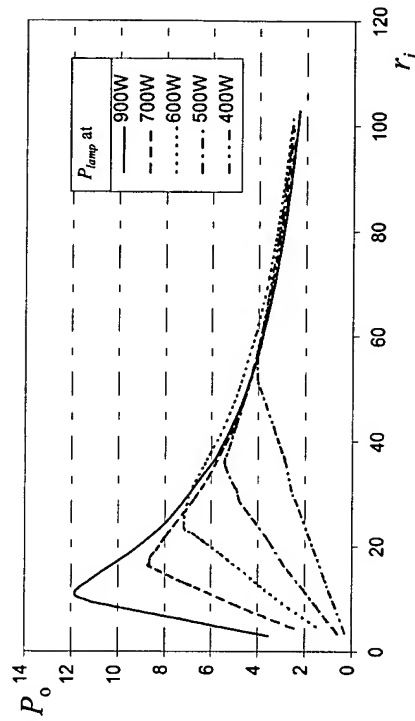


Fig. 5 Experimental setup for the solar panel.

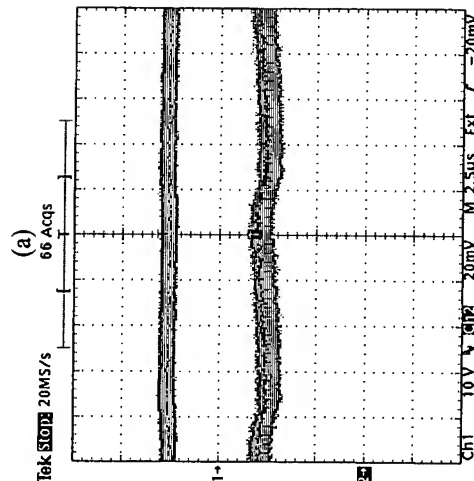
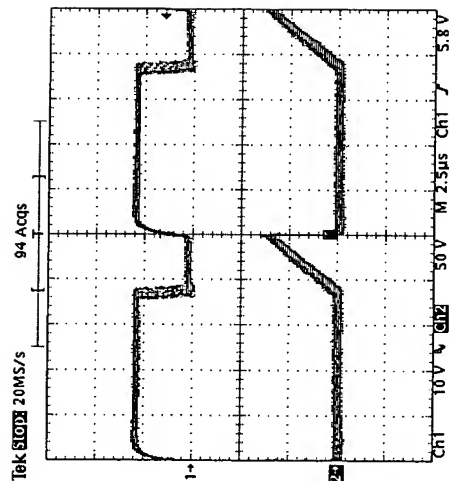


(a)



(b)

Fig. 6 Solar panel characteristics at different  $P_{lamp}$ . (a)  $i_g$  versus  $v_g$ . (b)  $P_o$  versus  $r_i$ .



(b)

Fig. 7 Detailed experimental waveforms of the SEPIC converter. (a) Ch1: gate signal, 10V/div; Ch2: switch voltage stress, 50V/div. (b) Ch1: input voltage, 10V/div; Ch2: input current, 0.5A/div.

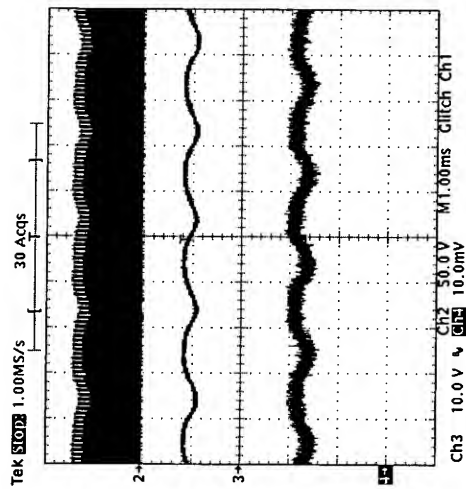
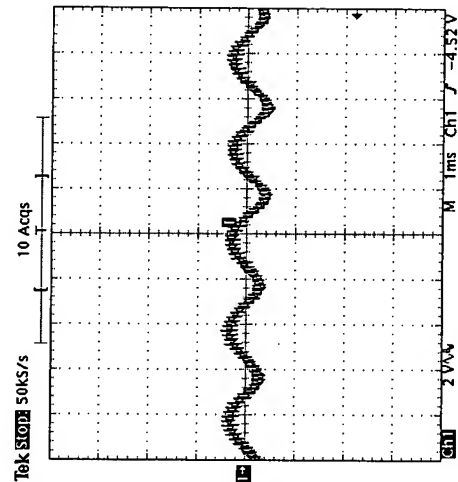
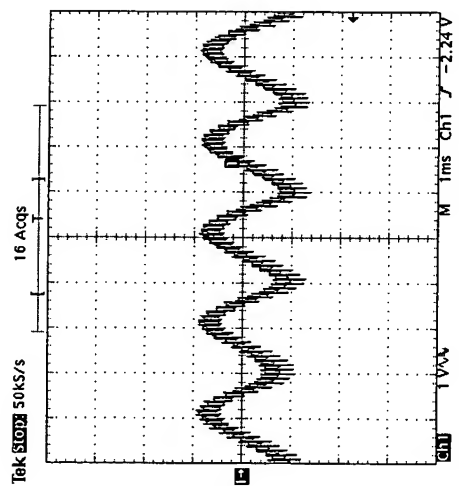


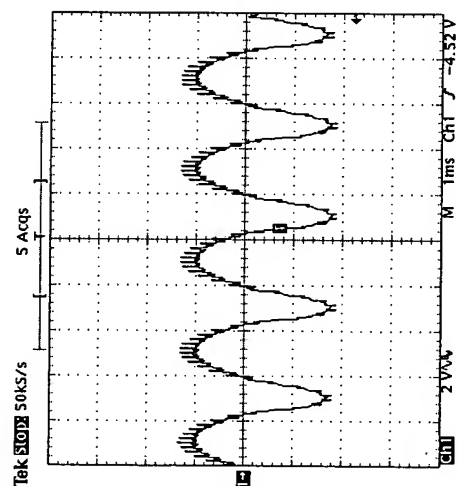
Fig. 8 Experimental waveforms of the SEPIC converter. Ch2: switch voltage stress, 50V/div; Ch3: input voltage, 10V/div; Ch4: input current, 0.5A/div.



(a)



(b)



(c)

Fig. 9 Waveform of  $\delta \hat{v}_i$  with respect to different value of  $\mathfrak{R}$ . (a)  $\mathfrak{R} = 0.02$ . (b)  $\mathfrak{R} = 0.05$ . (c)  $\mathfrak{R} = 0.1$ .

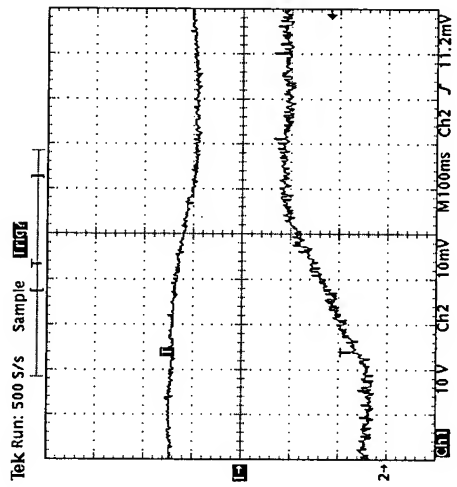


Fig. 10 Transient waveforms of the SEPIC converter subject to  $P_{lamp}$  changed from 500W to 900W. Ch1: input voltage, 10V/div. Ch2: input current, 0.5A/div.

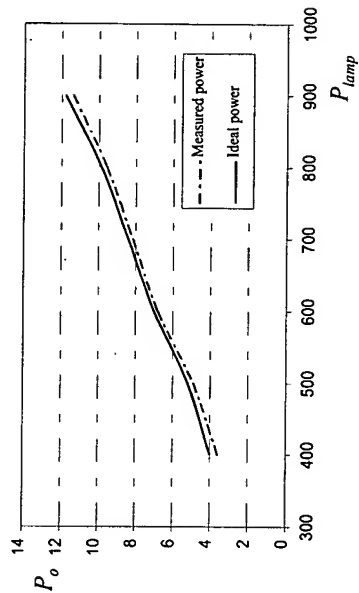


Fig. 11 Comparison of maximum solar panel output power using proposed method and the ideal ones in Fig. 6(b), under different  $P_{lamp}$ .

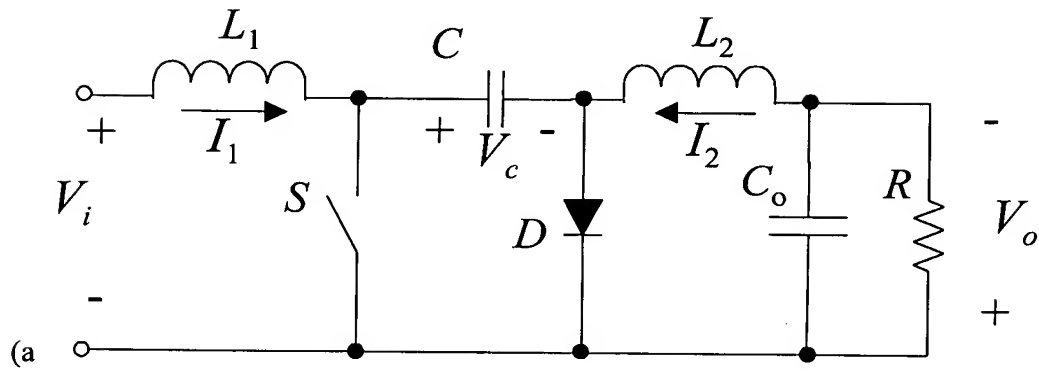


Fig. 12 Circuit diagram of the Cuk converter.

10005210-120401

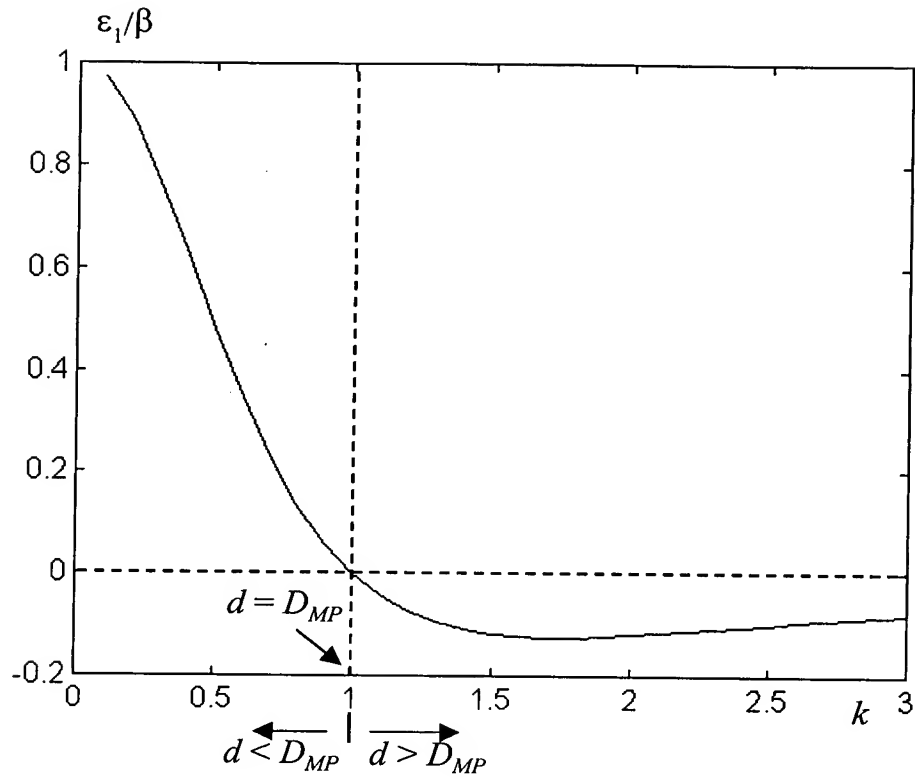


Fig. 13 Relationships between  $\epsilon_1 / \beta$  and  $k$ .

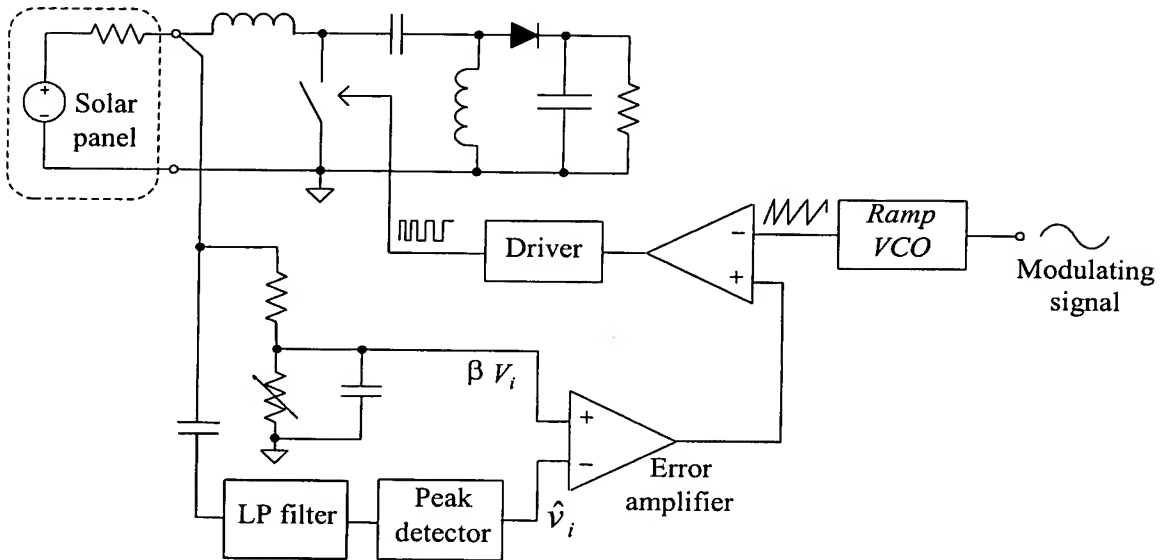


Fig. 14 The proposed MPP tracking method.

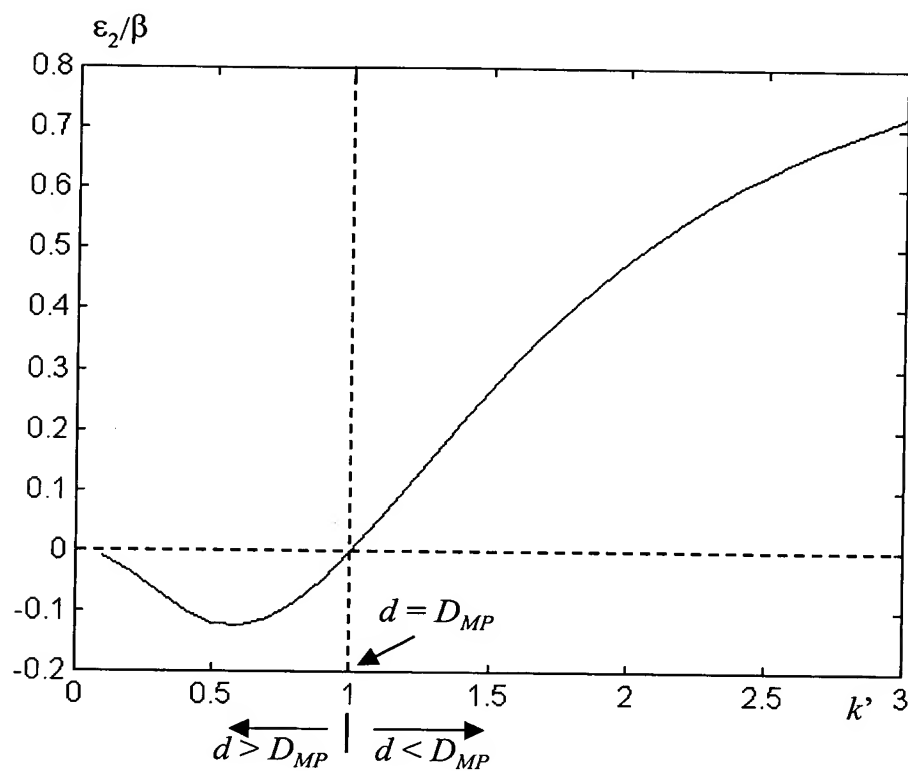


Fig. 15 Relationships between  $\epsilon_2/\beta$  and  $k'$ .

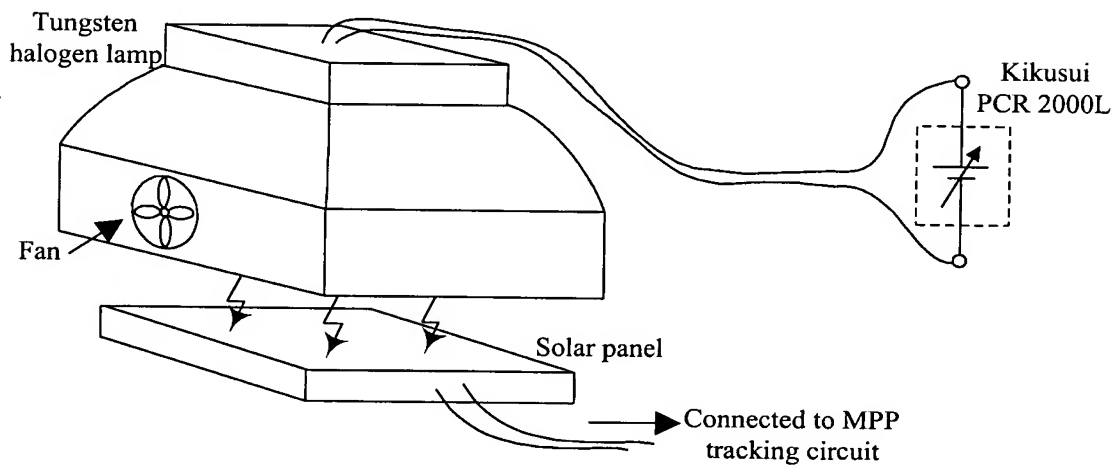


Fig. 16 Experimental setup for studying the proposed MPP tracking technique.

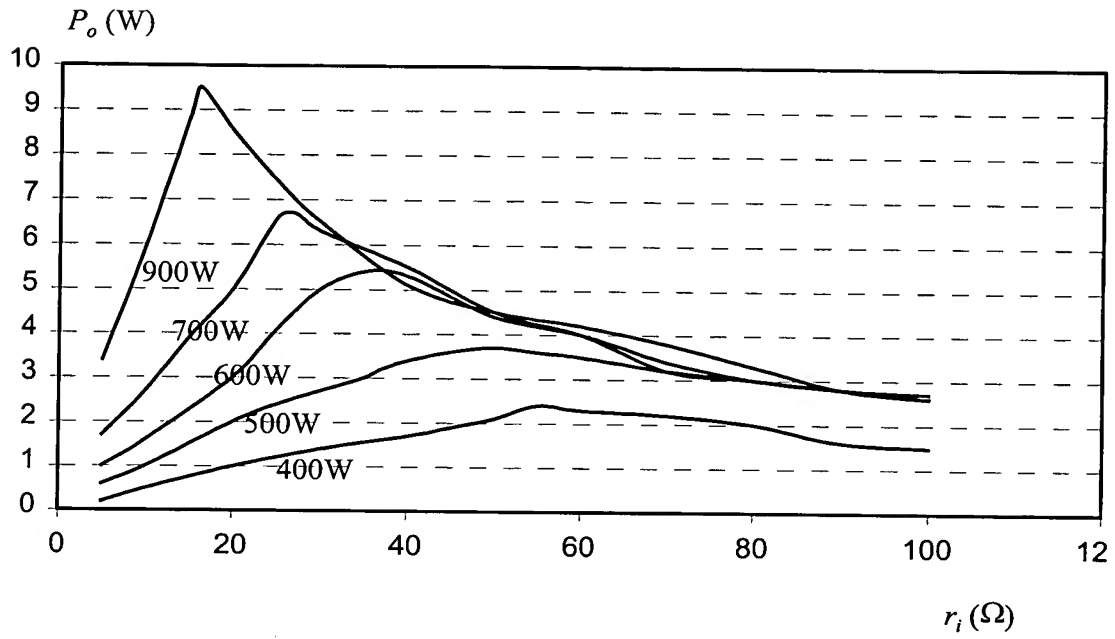
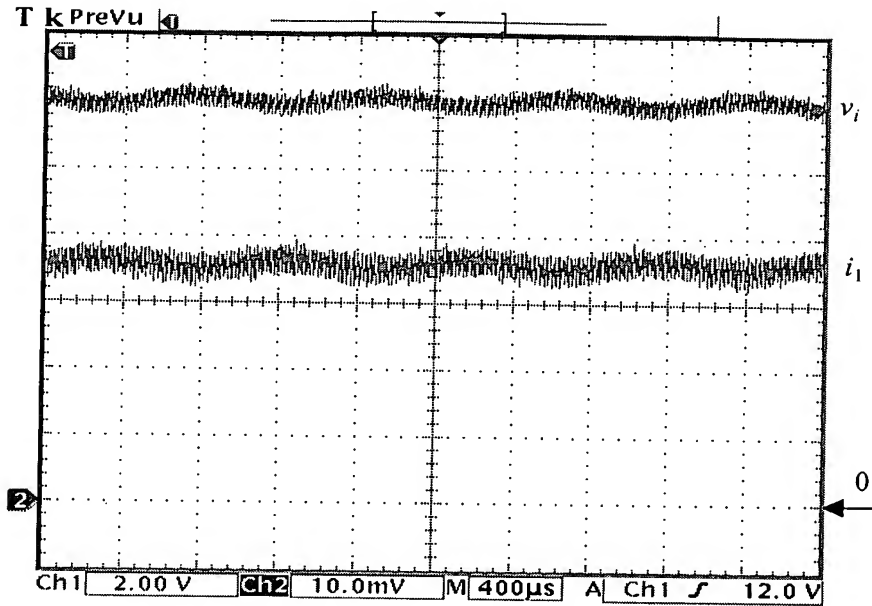


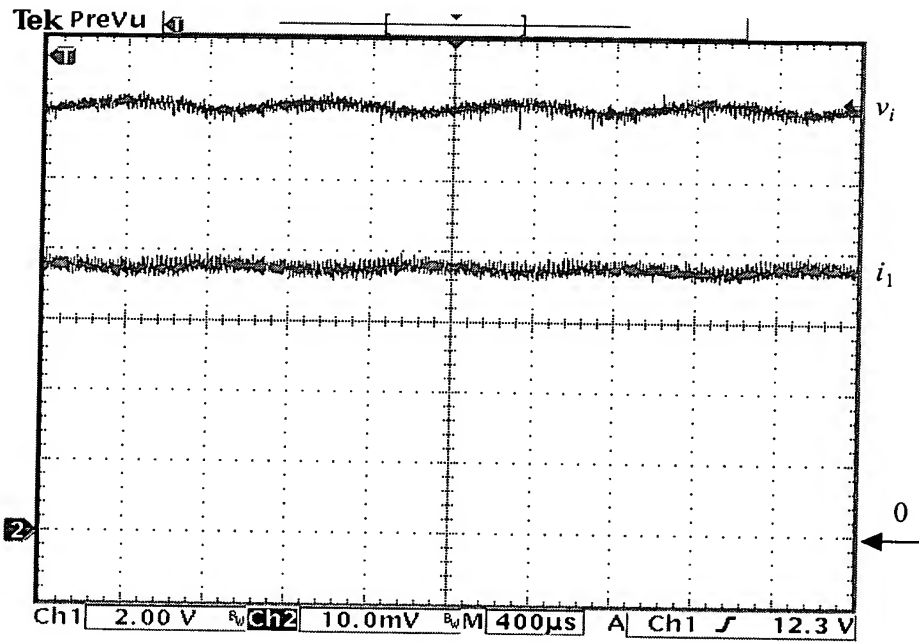
Fig. 17.  $P_o - r_i$  characteristics of the solar panel at different  $P_{lamp}$ .

10005210-120401



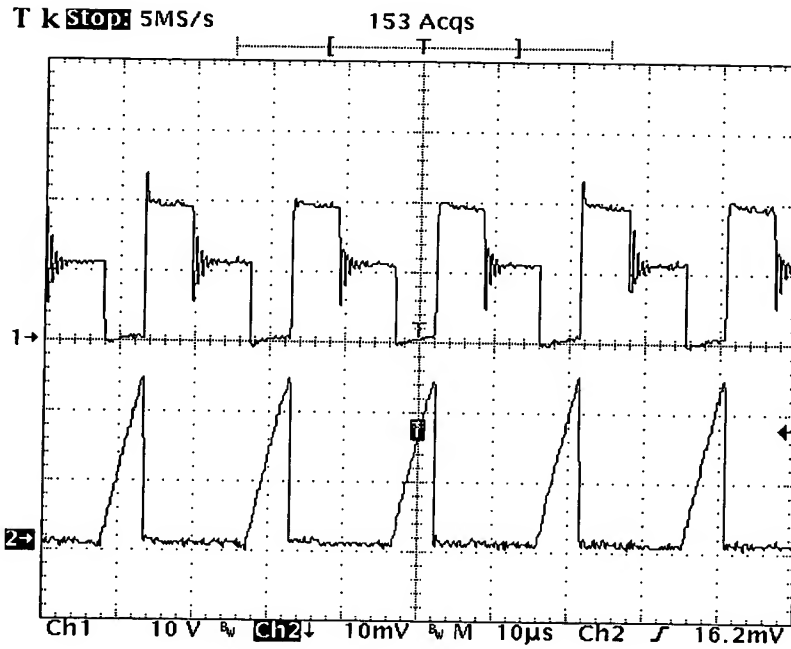


(a) DICM. ( $v_i$ : 2V/div.  $i_l$ : 0.2A/div.)

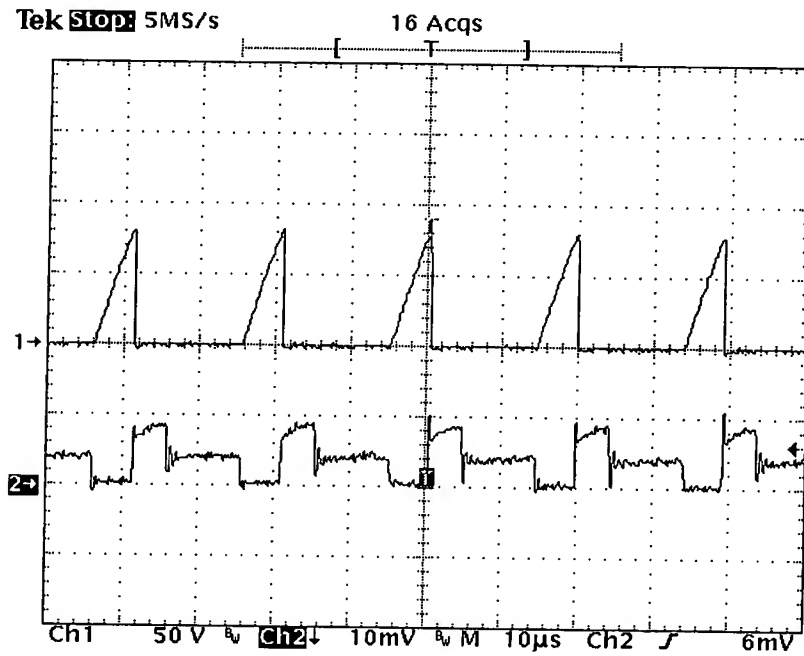


(b) DCVM. ( $v_i$ : 2V/div.  $i_l$ : 0.2A/div.)

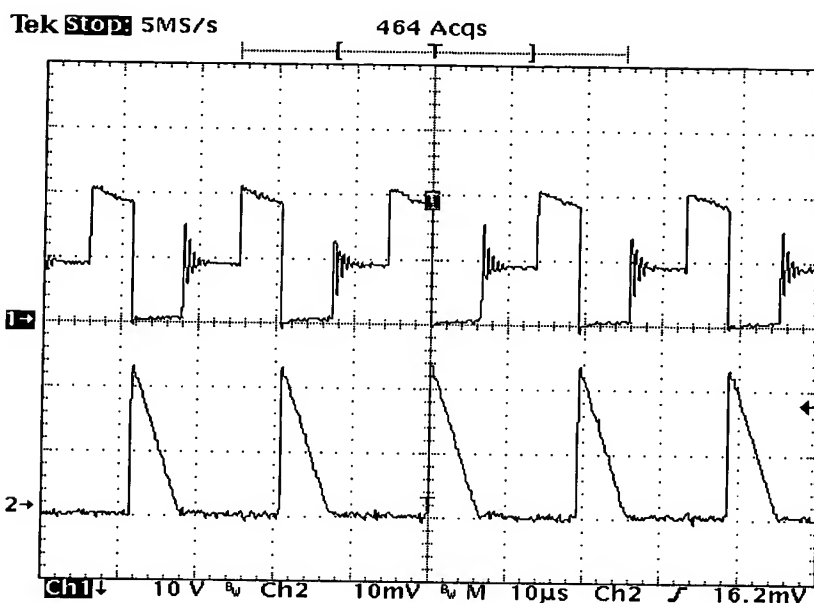
Fig.18. Experimental waveforms of  $v_i$  and  $i_l$  of the two SEPIC prototypes at the MPP when  $P_{lamp}$  equals 900W.



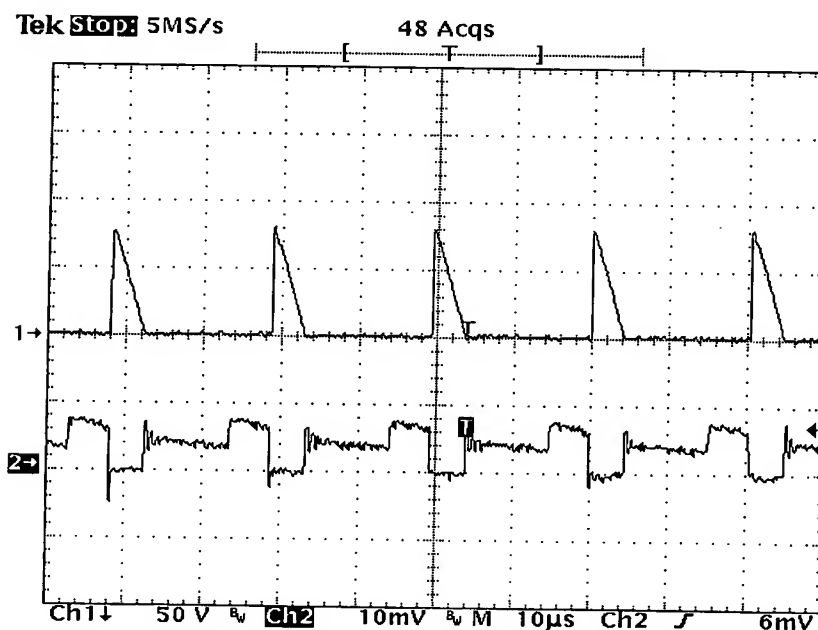
(a) Voltage and current stress on  $S$  in DICM. (Ch1: 10V/div. Ch2: 2A/div.)



(a) Voltage and current stress on  $S$  in DCVM. (Ch1: 50V/div. Ch2: 2A/div.)

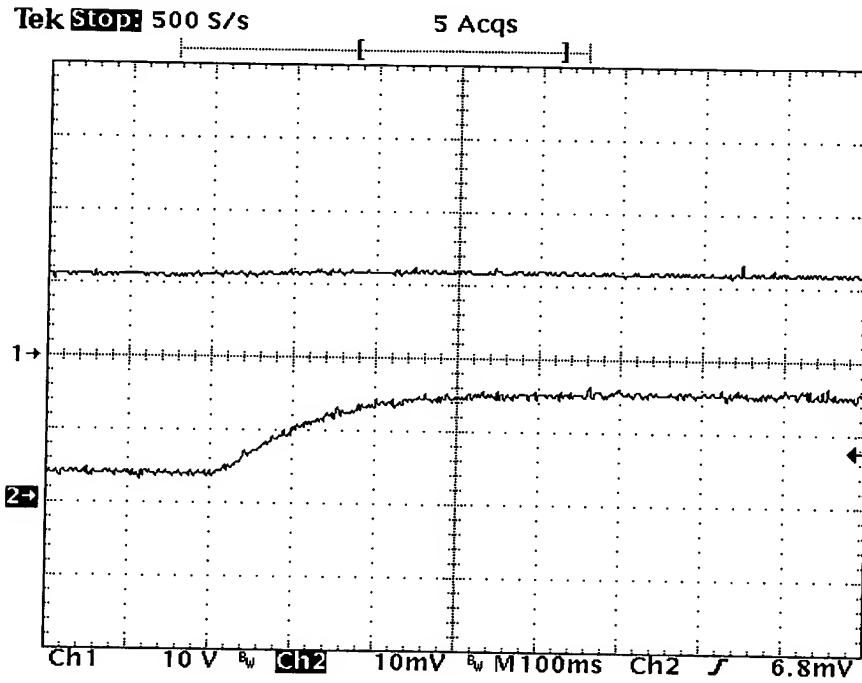


(c) Voltage and current stress on  $D$  in DICM. (Ch1: 10V/div. Ch2: 2A/div.)

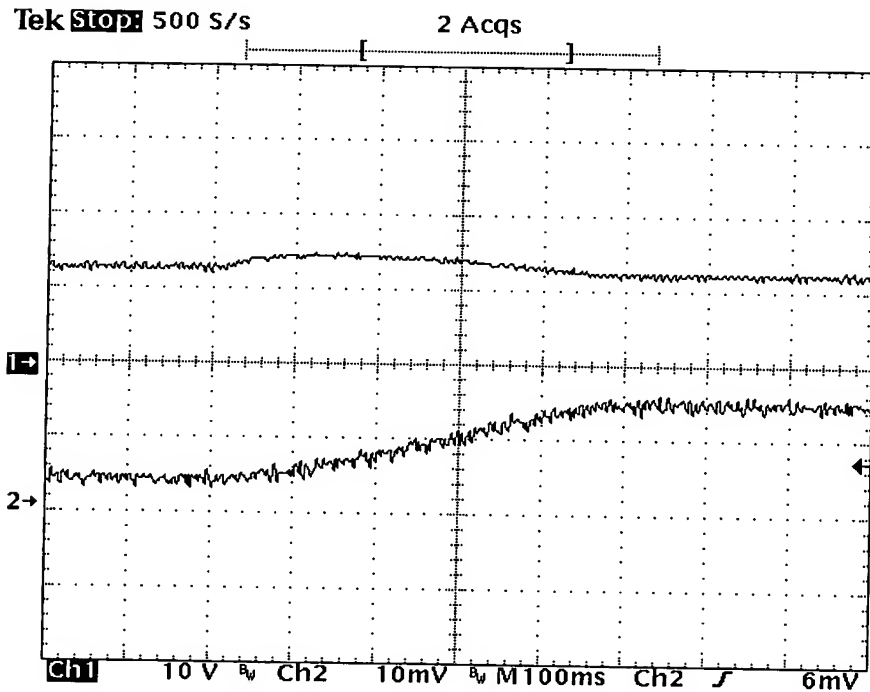


(d) Voltage and current stress on  $D$  in DCVM. (Ch1: 50V/div. Ch2: 2A/div.)

Fig.19. Experimental voltage and current stresses on  $S$  and  $D$ . (Timebase: 10μs/div)



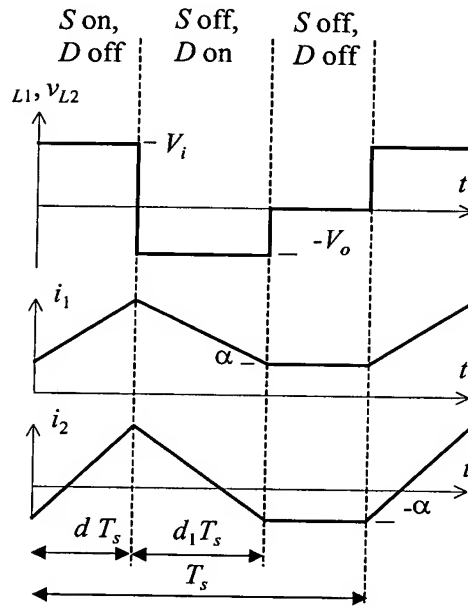
(a) DICM.



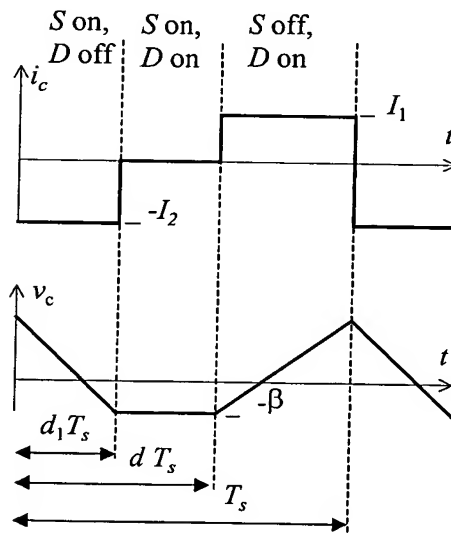
(b) DCVM.

Fig. 20. Experimental waveforms of the SEPIC converters when  $P_{lamp}$  is subject to a change from 400W to 900W. (Ch1:  $V_i$ , 10V/div. Ch2:  $I_i$ , 0.5A/div.)

10005210-120401



(a) Voltage and current waveforms of  $L_1$  and  $L_2$  in DICM.



(b) Current and voltage waveforms of  $C$  in DCVM.

Fig. 21 Key waveforms of SEPIC and Cuk converter.